ELECTRONIC SUPPLIMENTARY INFORMATION

Effect of point mutations on the ultrafast photo-isomerization of Anabaena Sensory Rhodopsin

D. Agathangelou[a], Y. Orozco-Gonzalez[a], M. del Carmen Marín[b], P. P. Roy[c], J.Brazard[a], H. Kandori[d], K-H. Jung[e], J.Leonard[a], T. Buckup[c], N. Ferré[f], M.Olivucci[b,g,h], and S.Haacke[a,†]

a. University of Strasbourg, CNRS, Inst. de Physique et Chimie des Matériaux de Strasbourg, 67034 Strasbourg, France.
b. Department of Biotechnology, Chemistry e Pharmacy, Università di Siena, via A. Moro 2, I-53100 Siena, Italy.
c. Physikalisch-Chemisches Institut, Ruprecht-Karls Universität Heidelberg, 69120 Heidelberg, Germany.
d. Department of Frontier Materials, Nagoya Institute of Technology, Showa-ku, Nagoya 466-8555, Japan
e. Department of Life Science and Institute of Biological Interfaces, Sogang University, Shinsu-Dong 1, Mapo-Gu, Seoul 121-742, South Korea
f. Aix-Marseille Université, CNRS, ICR, 13284 Marseille, France
g. Department of Chemistry, Bowling Green State University, Bowling Green, Ohio 43403, United States
h. USIAS Institut d'Études Avanceés, University of Strasbourg, 67083 Strasbourg, France

† Corresponding author: haacke@unistra.fr.

CONTENT

1. Molecular structure of the retinal binding pocket and mutated amino acids

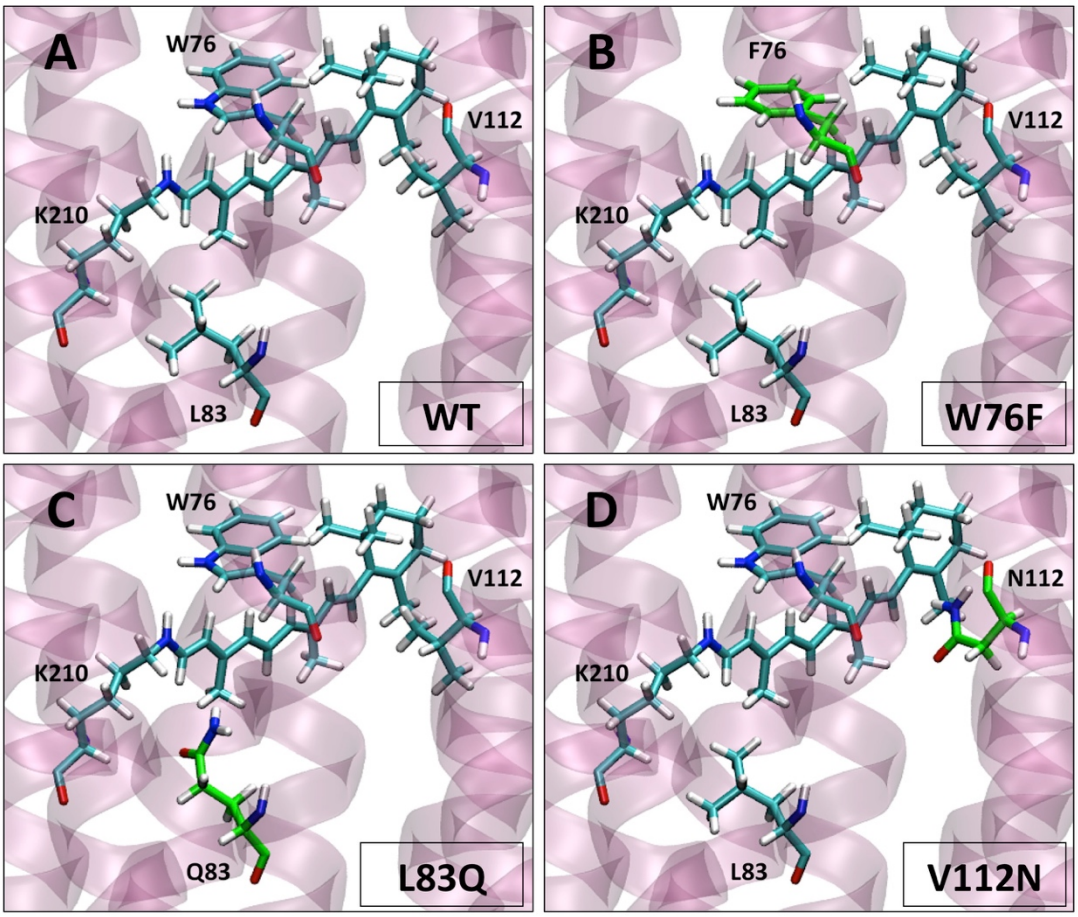

Figure S0: Molecular structures of dark-adapted ASR wild-type (A) and the three mutants studied, W76F (B), L83Q (C), and V112N (D). In the latter, the mutated residues are highlighted in green. All protein structures are computed using the ARM protocol [1] , and the software packages GROMACS 4.5.5 and MOLCAS 8.1/TINKER 6.3. for the QM/MM calculations. Figures of the protein snapshots were generated with VMD 1.9.2.

2. Computation of S_0-S_1 transition energies of the PSBR

a) Details of the computational results

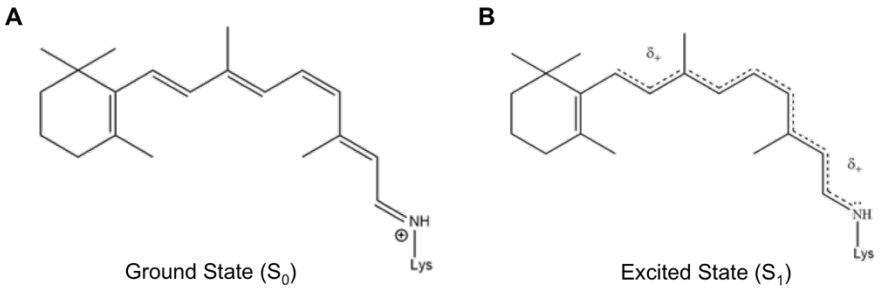

Figure S1: Electronic distribution of (A) ground state and (B) first excited state. In S0, the protonated Schiff base (PSB) linkage of Lys and the retinal chromophore is protonated. Photo-excitation in S_1, and the subsequent C=C bond length alternation lead to a partial charge transfer of the positive charge towards the β-ionone ring.

Table S1: Observed vs computed vertical excitation energies $\Delta E_{S1\text{-}S0}$ (kcal/mol) and Maximum Absorption Wavelengths (λ_{max}) for ASR WT and their mutants V112N, W76F, L83Q and L83Q* modified, ARM models computed at CASPT2/CASSCF(12,12)/6-31G*/AMBER level of theory. Oscillator strength and standard deviation are also shown.

Sample	State	Observed $\Delta E_{S1\text{-}S0}$ (λ_{max})	Computed $\Delta E_{S1\text{-}S0}$ (λ_{max})	f_{Osc}	DES.ST
WT	**AT**	51.9 (550)	53.5 (534)	1.14	1.0218
	13C	53.2 (537)	54.5 (526)	1.05	0.6400
V112N	**AT**	53.7 (532)	55.6 (513)	1.18	0.0483
	13C	54.2 (527)	55.8 (512)	1.10	0.1429
W76F	**AT**	54.0 (529)	56.1 (509)	0.98	0.5643
	13C	55.6 (514)	57.3 (498)	0.96	0.3534
L83Q	**AT**	55.3 (517)	53.6 (533)	1.16	1.0235
	13C	54.6 (523)	54.4 (524)	0.91	0.2478
L83Q*	**AT**	55.3 (517)	56.9 (502)	1.13	1.0345
	13C	54.6 (523)	57.6 (496)	0.99	0.3892

b) On the S_0 energy of the L83Q model

As outlined in the main text, the discrepancy with respect to experiments is related to the orientation of the O-H dipole moment of the Glu83 residue towards the Schiff base nitrogen (see fig. S3). The QM/MM model generated automatically by ARM protocol [1] orients this dipole with the positive end facing the SB (Fig. S2A), leading to destabilization of the ground state (S_0). However, a second minimum of the total free energy is found for an orientation of the O-H dipole, with the negative end pointing towards the protonated SB nitrogen (L83Q*, see fig. S2B), thus stabilizing S_0, and generating a blue-shift of λ_{max} similar to the experimental value. Table S2 and fig. S3 show the differences between the two models. However, the LA effect is not predicted in the right order.

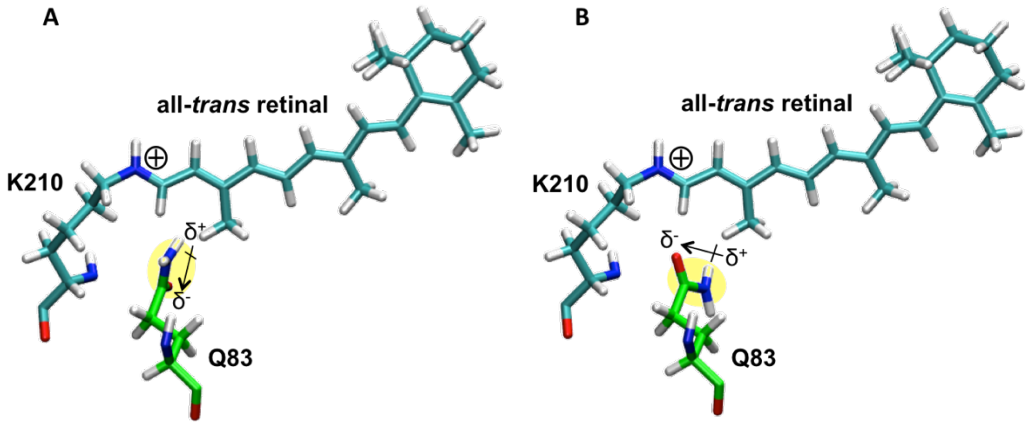

Figure S2: Comparison between the orientation of the dipolar moment for the L83Q mutant generated by (A) ARM protocol and (B) the manual modification L83Q*.

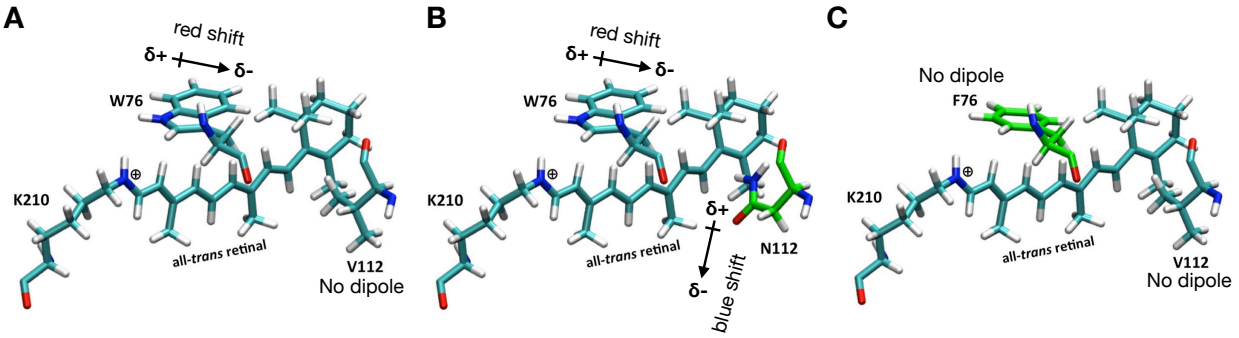

Figure S3: Comparison between ASRAT retinal chromophore and residues 112 and 76 in (A) WT model, (B) V112N mutant and (C) W76F mutant

Table S2: Computed energies (a.u.) of ground state (S_0) and first excited state (S_1) computed at CASPT2/CASSCF(12,12)/6-31G*/AMBER level for L83Q single mutant for the ARM models. The difference energies (kcal/mol) between WT and mutant for S_0 and S_1 are also shown.

Sample	State	Computed E_{S0} (a.u.)	Computed E_{S1} (a.u.)	ΔE_{S0} L83Q-L83Q* (kcal/mol)	ΔE_{S1} L83Q-L83Q* (kcal/mol)
L83Q	AT	-872.01516566	-871.92974105	15.5	12.1
	AT*	-872.03986273	-871.94902348		
	13C	-872.01403928	-871.9273348	11.4	8.2
	13C*	-872.03215695	-871.9403348		

*Manual change of residue Q83's orientation

Table S3: Computed energies (a.u.) of ground state (S_0) and first excited state (S_1) computed at CASPT2/CASSCF(12,12)/6-31G*/AMBER level for ASR WT and their mutants V112N and W76F. The difference energies (kcal/mol) between WT and mutant for S_0 and S_1 are also shown.

Sample	State	Computed E_{S0} (a.u.)	Computed E_{S1} (a.u.)	ΔE_{S0} WT-Mutant (kcal/mol)	ΔE_{S1} WT-Mutant (kcal/mol)
WT	**AT**	-872.01156040	-871.92575135		
	13C	-872.01764596	-871.93093400		
V112N	**AT**	-872.00746983	-871.91875825	+2.6	+4.4
	13C	-872.01591336	-871.92714670	+1.1	+2.4
W76F	**AT**	-872.00652936	-871.91642845	+3.2	+5.9
	13C	-872.01176479	-871.92028250	+3.7	+6.7

3. Time-resolved vibrational spectroscopy

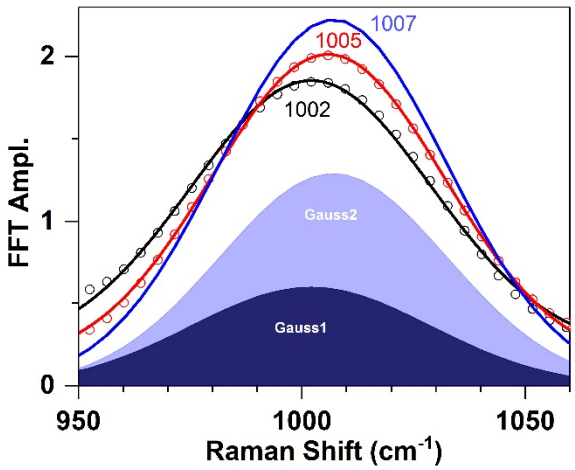

Figure S4: Gaussian fit of CH_3 rocking mode of GS ASR in dark (black curve) and light adapted (red curve) conditions. Dark adapted GS was fitted with a single Gaussian. For light adapted GS, a double Gaussian constrained fit was performed fixing the center and width of first Gaussian (Gauss1) as obtained by fitting the DA GS. The Gaussians required to fit the LA GS line shape are shown as filled curves. The reconstructed pure-13C spectrum is represented as blue line.

Table S3: Parameters obtained by Gaussian fitting of C=C mode of DA GS and constrained double Gaussian fitting of same mode of LA ASR shown in Fig. X3.

	Gauss1			Gauss2		
	Amp.	**Centre frequency (cm^{-1})**	**Width (cm^{-1})**	**Amp.**	**Centre frequency (cm^{-1})**	**Width (cm^{-1})**
DA GS (C=C stretching)	0.54 ±0.003	1530 ±0.4	68 ±6	-	-	-
LA GS (C=C stretching)	0.08 ±0.03	1530 (fixed)	68 (fixed)	0.19 ±0.02	1540 ±1.0	52 ±5
DA GS (CH_3 rocking)	0.16 ±0.004	1002 ±0.3	64 ±5	-	-	-

LA GS **(CH_3 rocking)**	0.06 ±0.003	1002 (fixed)	64 (fixed)	0.13 ±0.002	1007 ±0.2	57 ±4

Table S4: Frequencies of major vibrational modes obtained by non-resonant DFWM and Pump-DFWM probed at 610 nm at a delay T=100 ps. All frequencies are given in cm^{-1}.

	CH_3 rocking	Fingerprint region	C=C stretching
DA GS	1003	1165, 1230	1530
LA GS	1007	1180, 1300	1539
DA @ T=100 ps	1003	1170, 1245	1535
LA @ T=100 ps	1007	1174, 1305	1532

4. Transient absorption spectroscopy

We report here the kinetic traces for stimulated emission of the AT isomer in the three mutants obtained after data averaging in the spectral regions of 700-721 nm. These regions represent pure SE without any contribution from GSB or ESA:

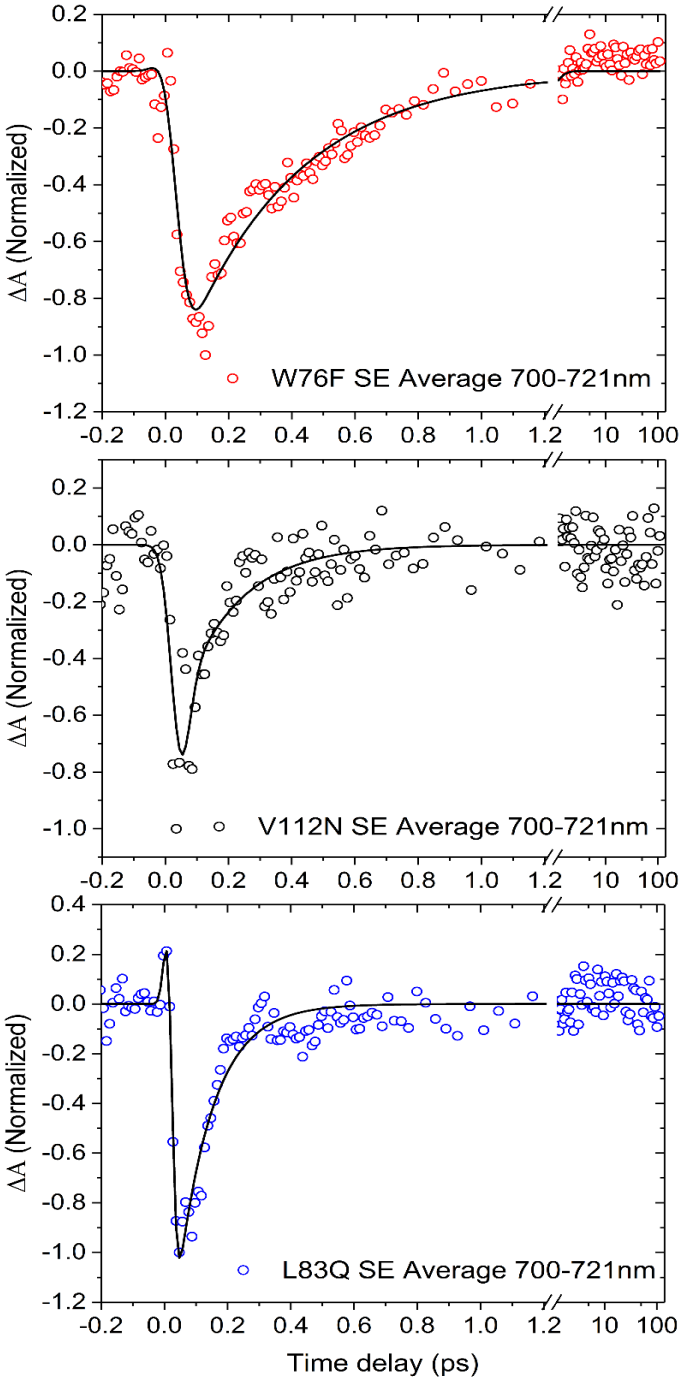

Figure S5: Normalized stimulated emission kinetic traces of AT isomers in the 3 mutants averaged from 700-721nm. Black solid lines represent the mono-exponential fits of the data. Fit parameters are given in the main text. The SNR in the V112N data (middle panel) is not sufficient to determine a possible 2nd slower decay time in the 0.3-0.8 ps range.

5. References

[1] F. Melaccio, M. Del Carmen Marin, A. Valentini, F. Montisci, S. Rinaldi, M. Cherubini, X. Yang, Y. Kato, M. Stenrup, Y. Orozco-Gonzalez, N. Ferre, H. L. Luk, H. Kandori and M. Olivucci, *J Chem Theory Comput*, 2016, **12**, 6020-6034